

OPEN ACCESS

Towards ^{26}Na via (d,p) with SHARC and TIGRESS and a novel zero-degree detector

To cite this article: G L Wilson *et al* 2012 *J. Phys.: Conf. Ser.* **381** 012097

View the [article online](#) for updates and enhancements.

You may also like

- [Diffuse Ionized Gas in Simulations of Multiphase, Star-forming Galactic Disks](#)
Erin Kado-Fong, Jeong-Gyu Kim, Eve C. Ostriker et al.
- [Pressure-regulated, Feedback-modulated Star Formation in Disk Galaxies](#)
Eve C. Ostriker and Chang-Goo Kim
- [Cosmic-Ray Transport in Varying Galactic Environments](#)
Lucia Armillotta, Eve C. Ostriker, Yan-Fei Jiang et al.



The
Electrochemical
Society

Advancing solid state &
electrochemical science & technology



DISCOVER
how sustainability
intersects with
electrochemistry & solid
state science research



Towards ^{26}Na via (d,p) with SHARC and TIGRESS and a novel zero-degree detector

G L Wilson¹, W N Catford¹, C Aa Diget², N A Orr³, P Adsley²,
H Al-Falou⁴, R Ashley⁵, R A E Austin⁶, G C Ball⁴, J C Blackmon⁷,
A J Boston⁵, H J Boston⁵, S M Brown¹, A A Chen⁸, J Chen⁸,
R M Churchman⁴, D S Cross⁴, J Dech⁴, M Djongolov⁴, T E Drake⁹,
U Hager⁴, S P Fox², B R Fulton², N Galinski⁴, A B Garnsworthy⁴,
G Hackman⁴, D Jamieson¹², R Kanungo⁶, K Leach¹², J-P Martin¹⁰,
J N Orce⁴, C J Pearson⁴, M Porter-Peden¹¹, F Sarazin¹¹, S Sjue⁴,
C Sumithrarachchi⁴, C E Svensson¹², S Triambak⁴, C Unsworth⁵,
R Wadsworth², S J Williams⁴ and the TIGRESS collaboration.

¹ Department of Physics, University of Surrey, Guildford, Surrey. GU2 7XH, UK

² Department of Physics, University of York, York, YO10 5DD, UK

³ Laboratoire de Physique Corpusculaire, ENSICAEN et Université de Caen, IN2P3-CNRS, 14050 Caen Cedex, France

⁴ TRIUMF, 4004 Wesbrook Mall, Vancouver, BC, V6T 2A3, Canada

⁵ Department of Physics, University of Liverpool, Liverpool, L69 3BX, UK

⁶ Department of Astronomy and Physics, St Mary's University, Halifax, NS, B3H 3C3, Canada

⁷ Department of Physics and Astronomy, Louisiana State University, Baton Rouge, LA 70803, USA

⁸ Department of Physics and Astronomy, McMaster University, Hamilton, ON, L8S 4M1, Canada

⁹ Department of Physics, University of Toronto, Toronto, Ontario, M5S 1A7, Canada

¹⁰ Département de Physique, Université de Montréal, Montréal, QC, H3C 3J7, Canada

¹¹ Department of Physics, Colorado School of Mines, Golden, CO 80401, USA

¹² Department of Physics, University of Guelph, Guelph, ON, N1G 2W1, Canada

E-mail: g.wilson@surrey.ac.uk

Abstract. Nucleon transfer experiments have in recent years begun to be exploited in the study of nuclei far from stability, using radioactive beams in inverse kinematics. New techniques are still being developed in order to perform these experiments. The present experiment is designed to study the odd-odd nucleus ^{26}Na which has a high density of states and therefore requires gamma-ray detection to distinguish between them. The experiment employed an intense beam of up to 3×10^7 pps of ^{25}Na at 5.0 MeV/nucleon from the ISAC-II facility at TRIUMF. The new silicon array SHARC was used for the first time and was coupled to the segmented clover gamma-ray array TIGRESS. A novel thin plastic scintillator detector was employed at zero degrees to identify and reject reactions occurring on the carbon component of the (CD)₂ target. The efficiency of the background rejection using this detector is described with respect to the proton and gamma-ray spectra from the (d,p) reaction.

1. Introduction

One of the proposed areas of study using SHARC [1], a new highly-segmented silicon array, is the evolution of structure in the region of $N = 16$ as revealed by neutron transfer reactions. Such

experiments can highlight the states carrying significant fractions of the single-particle strength, in the populated nuclei. The ISAC-II facility at TRIUMF [2] is ideal for this type of study, as it is able to produce intense sodium beams in the relevant range of energies ($\sim 5 - 10$ MeV/nucleon), and it also houses TIGRESS [3, 4], a highly efficient germanium array. The design of SHARC is an evolution of the TIARA array [5], which achieved success in investigating the changing shell structure of light nuclei via transfer reactions [6].

2. Experimental details

The radioactive ion-beam facility ISAC-II at the TRIUMF laboratory was employed for the study of the $^{25}\text{Na}(d,p)^{26}\text{Na}$ reaction in inverse kinematics. A primary beam of 500 MeV protons impinged on a silicon carbide target, and up to 3×10^7 pps of ^{25}Na at 5 MeV/nucleon was provided by ISAC-II. The beam was incident upon a 0.5 mg/cm^2 CD_2 target, located at the centre of the SHARC and TIGRESS arrays. Signals from all active detectors were recorded whenever any of the silicon detectors triggered. Downstream of the target, a thin scintillator detector (the “TRIFOIL”) was mounted on the beam axis and immediately behind an aluminium stopping foil. The foil thickness was chosen so as to stop any slower, higher atomic number nuclei originating from fusion-evaporation reactions induced by the beam on the ^{12}C component of the target. The arrangement and operation of the detectors are described in more detail, below.

2.1. SHARC

The SHARC array comprises highly segmented Double-Sided Silicon Strip Detectors (DSSSDs) providing a large angular coverage. In the present experiment, the setup consisted of two boxes of four DSSSDs, one mounted upstream of the target and the other downstream, with a gap at 90° to the beam direction. The target mechanism enters through this gap and allows the use of several targets. There is also space for both upstream and downstream annular CD-detectors [7]. The downstream box was instrumented on one face only (covering $135^\circ < \phi < 225^\circ$) and comprised of a $\Delta E - E$ telescope, with a DSSSD and a pad detector (unsegmented) mounted back to back. The active area of silicon of each detector measures $48 \times 72 \text{ mm}$ and is offset on the PCB so that the active area reaches the very edge on two sides, as shown in Fig. 1a. This, coupled with the ‘windmill’ configuration (Fig. 1b), has the advantage of maximising the angular coverage. The present experiment was mounted with the active area giving optimal coverage close to 90° . A single CD-detector was mounted, at the most backward angles.

The DSSSDs are segmented into twenty-four 3 mm horizontal strips parallel to the z-axis and

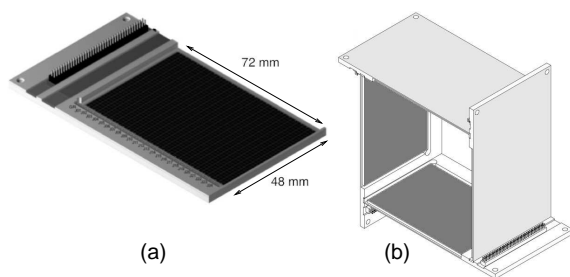


Figure 1. (a) the bespoke design of the box detector; (b) the windmill configuration of mounting the detectors [1]

forty-eight 1 mm vertical strips perpendicular to the z-axis. The two boxes cover angles from 34.8° to 149.3° , with a gap from 81.8° to 95.7° . In this work, four DSSSDs which were $1000 \mu\text{m}$ thick were mounted in the upstream box along with an upstream CD array of thickness $400 \mu\text{m}$. The CD array is made of four individually cabled quadrants, each segmented into sixteen rings and twenty-four sectors [7]. These double sided detectors covered the angles 149.3° to 172.8° . The ΔE detector in the downstream box was $140 \mu\text{m}$ thick, with a $1500 \mu\text{m}$ thick pad detector behind it. Individual strips are connected by multiwire cable to purpose-built preamplifiers

mounted immediately outside of the target chamber on the downstream side. The preamplifier outputs were transported 20 metres via SCSI-5 cables to the same model of TIG10 modules as used for digitizing TIGRESS signals [8]. Further details concerning SHARC may be found in ref. [1].

2.2. TIGRESS

TIGRESS, the TRIUMF-ISAC Gamma-Ray Escape-Suppressed Spectrometer, is a Hyper-Pure Germanium (HPGe) array. It consists of up to sixteen HPGe detectors that can be mounted in rings orientated at $\theta = 45^\circ$, 90° and 135° around the target. The SHARC target chamber excludes access to the 45° positions, so the eight detectors available at the time of the experiment were mounted with four in each of the other rings. Each clover consists of four individual closed-ended coaxial HPGe crystals which are packed into a common cryostat, with tapering at the front of the crystal to allow for close packing. The crystals are n-type and have approximately 40% relative efficiency. Each clover has 32-fold segmentation: each of its four crystals has four quadrants and there is a lateral segmentation at $z = 31$ mm, where $z = 0$ corresponds to the front of the crystal. The four rear segments in each clover reduce the uncertainty in the angle of emission of the γ -ray, by providing 3D localisation [9]. Each clover in the TIGRESS array is flanked by four Bismuth-Germanate shields, all of which were mounted for this experiment. Coupled with a CsI(Tl) plug behind the clover, the suppression shields have twenty-fold segmentation [4] to allow for full Compton suppression. Titanium collimators are attached to the front of the clovers, to prevent any gamma rays directly striking the BGO shields. The front face of the clovers were 14 cm from the target.

2.3. TRIFOIL

Downstream of SHARC and TIGRESS, an in-beam zero degree detector was mounted at a distance of 40 cm from the target. Whereas in previous experiments a spectrometer was employed at zero degrees [6], this was not available at ISAC-II and a simpler solution was required in order to distinguish between transfer reaction recoils and other products. Specifically, fusion-evaporation reactions induced on the carbon component of the target were expected to produce a significant and relatively isotropic background of light charged particles (mainly protons). The corresponding compound nuclei were typically slower moving and of higher Z than the beam and hence the (d,p) reaction products. An aluminium stopping foil was inserted in the beam path, with the thickness of $30\text{ }\mu\text{m}$ chosen to be just sufficient to stop the evaporation nuclei. The beam particles and the reaction products retained sufficient energy to pass easily through the thin plastic scintillator of the TRIFOIL detector and be transported to a shielded beam dump at a distance of ~ 2 metres.

The TRIFOIL detector is so named because it utilises three photomultiplier tubes, as shown in Fig. 2. The active area consists of a $10\text{ }\mu\text{m}$ thick BC400 plastic scintillator foil, with an active area 40×40 mm, mounted in a plexiglass frame that acts as a light guide. The foil thickness is optimised for good light output for the ions and energies considered here whilst inducing the minimum possible multiple scattering. For the TRIFOIL to trigger, at least two of the three photomultiplier tubes need to fire in coincidence. This allows the individual thresholds to be set at a level comparable with the noise, which is required for very low optical yield of such a thin scintillator foil.

The kinematics of the ejected protons were calculated, and it was found that the TRIFOIL could be mounted 40 cm behind the target and still span the entire cone of the reaction products for protons recorded backwards of 90° . The TRIFOIL was exposed to all beam particles, as the beam was transmitted through it before being incident upon the beam dump. The aluminium foil stopped the fusion-evaporation products, as discussed above. The alternative was to rely upon the timing of the TRIFOIL signal relative to the RF signal from ISAC-II to be able to distinguish

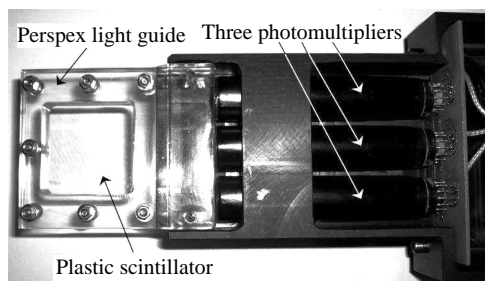


Figure 2. The TRIFOIL is shown, with its plexiglass frame and three photomultipliers.

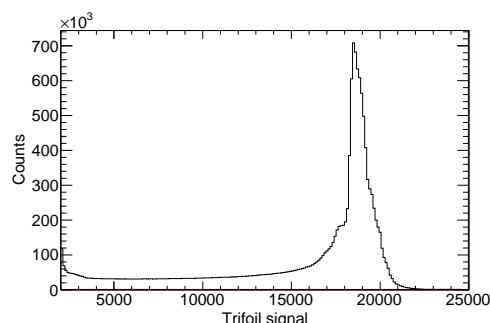


Figure 3. A typical TRIFOIL spectrum obtained by processing the stored logic signal for each event. The events in the peak correspond to the presence of a logic output from the TRIFOIL. A threshold of 15000 was set on this parameter to select (d,p) events.

the direct reaction products from the more slowly moving contaminants. This was rejected because it would have required a resolution of order 1 ns. At the time of the experiment, the width of the beam bunches could not be tuned to the required accuracy. A logic discriminator signal from the TRIFOIL indicated the presence of either a reaction product or a beam particle. The NIM output from the TRIFOIL coincidence unit was sent directly to the data acquisition system. Using the TIG10 modules, with the option of storing a selected part of the waveform, the region in time containing several beam bunches around the bunch of interest was stored. The bunch corresponding to genuine coincidences with the silicon trigger signal was identified and a simple algorithm developed to integrate the size of any NIM logic pulse that was present at that time.

A typical TRIFOIL spectrum is shown in Fig. 3. It has some structure due to the timing jitter relative to the integration region, which could be improved in future applications of the technique. An important feature of this method is that it is completely deadtime free. That is, a trace from the coincidence unit is always recorded and it is simply a matter of the analysis to determine whether the TRIFOIL signal was present at the correct time. This is in contrast to any system using a TAC or simple TDC.

3. TRIFOIL Efficiency

The TRIFOIL was developed originally at LPC Caen for use in experiments with fast fragmentation beams. The foil thickness is chosen according to the energy and charge of the relevant ions and the photomultiplier voltage is adjusted to optimise the efficiency. In the case of fragmentation beams the beam spot is extended, but the beam spot obtained from ISAC-II is only of order 1.5 mm diameter and this concentration of deposited energy can lead to a rapid degradation of the scintillation properties of the foil. However, the beam particles that do not cause reactions in the target are not of particular interest and this degradation is not a problem so long as it remains localised in the region of the beam spot and does not affect the production or collection of the light from elsewhere in the foil. The stable behaviour of the rest of the foil was verified by periodically moving the TRIFOIL position and comparing the count rate to that of an upstream beam intensity monitor. The efficiency of the TRIFOIL for tagging (d,p)

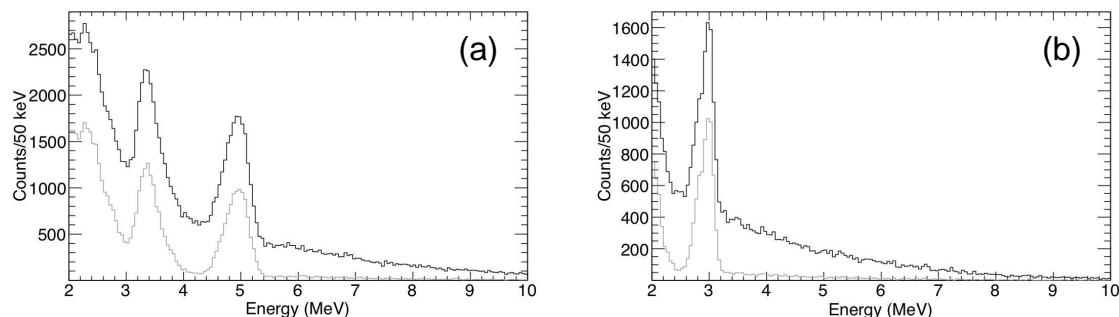


Figure 4. A comparison of proton reaction data with and without the TRIFOIL requirement laboratory angles: (a) $105^\circ < \theta < 107^\circ$, (b) $129^\circ < \theta < 131^\circ$. The grey line includes the TRIFOIL requirement.

reactions was investigated using proton energy spectra observed at various angles relative to the beam. Proton energy spectra projected for $\theta = 105 - 107^\circ$ and $\theta = 129 - 131^\circ$ are shown in Fig. 4. The measurement employed the highest energy proton peaks (at around 5 MeV and 3 MeV, respectively, in Figs. 4a and 4b). The fraction of background events that is nevertheless tagged by the TRIFOIL was measured using the area from above the peak, up to 10 MeV. As shown in Table 1, approximately 80% of the protons are tagged, and 90% of the underlying background is suppressed, so that the signal to background is improved by a factor of 10.

The efficiency was also measured for tagging the gamma rays recorded in coincidence with

Table 1. TRIFOIL efficiencies for the protons detected in SHARC and the associated background.

Angle Range (degrees)	$\Sigma_{Tri}/\Sigma_{noTri}$ Peak	$\Sigma_{Tri}/\Sigma_{noTri}$ Background
$105 < \theta < 107$	0.72 ± 0.01	0.11 ± 0.01
$129 < \theta < 131$	0.84 ± 0.01	0.11 ± 0.01

particles in SHARC. The spectrum from just one leaf of one clover was used, since the gamma rays from different origins will have different Doppler shifts. The spectrum acquired at 82° , from a clover centred at 90° , is shown in Fig. 5. Compton suppression and Doppler correction ($v/c = 0.091$) have been applied. In addition to genuine coincidences with direct reaction products, some fusion-evaporation transitions could be present as well as some random coincidences with gamma rays from the room background and the decay of scattered ^{25}Na beam particles. Table 2 shows the measured tagging efficiencies for gamma rays. The first point to notice is that the flat background arising from higher energy gamma rays is strongly suppressed: at 700 keV the rejection ratio is 6:1. Regarding the peaks, the gamma rays arising from (d,p) are tagged with an efficiency of typically 67%. Peaks arising from the radioactive decay of scattered ^{25}Na projectiles are randomly in coincidence with reaction particles and the TRIFOIL at a level of 11% (note that no fast timing information is presently included). Combining these figures with those for the protons, the peak-to-background ratio for gamma rays gated on proton peaks is improved by a factor of approximately 40 by using the TRIFOIL. In addition, gamma rays not arising from direct reactions are suppressed by a factor of 6 relative to reaction gamma rays. This ratio is similar for compound nuclear (CN) transitions and the decay of scattered

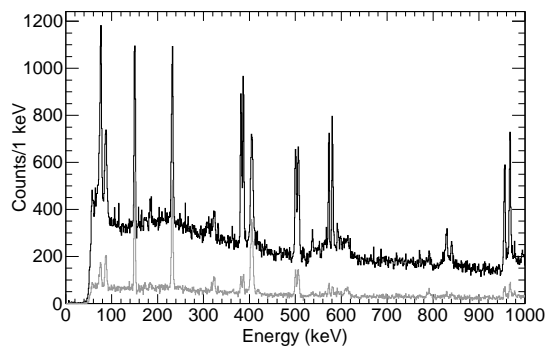


Figure 5. A gamma-ray spectrum at $\theta = 82^\circ$. The lighter spectrum has had the TRIFOIL condition applied, and it can be seen that both the background and some of the peaks are greatly reduced.

beam, implying that the aluminium stopping foil is highly effective. It is anticipated that a timing signal calculated from the TIG10 traces should improve the rejection of the random background.

Table 2. TRIFOIL efficiencies for the gamma rays detected in TIGRESS and the associated background.

E_γ (keV)	$\Sigma_{Tri}/\Sigma_{noTri}$	Identification	E_γ (keV)	$\Sigma_{Tri}/\Sigma_{noTri}$	Identification
151	0.69 ± 0.02	^{26}Na	385	0.12 ± 0.01	^{25}Na decay
233	0.61 ± 0.02	^{26}Na	577	0.09 ± 0.01	^{25}Na decay
407	0.67 ± 0.02	^{26}Na	835	0.10 ± 0.01	CN
503	0.26 ± 0.01	511 keV	961	0.13 ± 0.01	^{25}Na decay
700	0.16	background			

4. Summary

The new SHARC array has been found to work well for the study of direct reactions with radioactive beams at an intensity of up to 3×10^7 pps. The TRIFOIL, coupled with an aluminium stopper foil, has proven invaluable for separating the events arising from fusion-evaporation and direct reactions. In addition, the TRIFOIL improves the peak to background ratio in the energy spectrum of gamma rays observed in coincidence with particles, by a factor of approximately 40. Further analysis of the data is underway, to study the spectrum of states populated in ^{26}Na and to deduce the transferred angular momentum from the proton angular distributions.

References

- [1] Diget C Aa *et al* 2011 *J Inst. G* **6** P02005
- [2] Bricault P 2007 *Eur. Phys. J Special Topics* **150** 227-232
- [3] Garrett P E *et al* 2007 *Nucl. Instr. Meth. B* **261** 1084-1088
- [4] Schumaker M A *et al* 2007 *Nucl. Instr. Meth. A* **573** 157-160
- [5] Labiche M *et al* 2010 *Nucl. Instr. Meth. A* **614** 439-448
Catford W N *et al* 2005 *Eur. Phys. J.* **A25** s01 245-250
- [6] Catford W N *et al* 2010 *Phys. Rev. Lett.* **104** 192501
Fernández-Domínguez B *et al* 2011 *Phys. Rev. C* **84** 011301(R)
- [7] Ostrowski A N *et al* 2002 *Nuc. Instr. Meth. A* **480** 448-455
- [8] Martin J-P *et al* 2008 *IEEE Transactions on Nuclear Science* **55** 84-90
- [9] Scraggs H C *et al* 2005 *Nucl. Instr. Meth. A* **543** 431-440